ISSN:1984-2295

Revista Brasileira de Geografia Física

Homepage:https://periodicos.ufpe.br/revistas/rbgfe

Monitoring of degradation in the Caatinga biome in the semi-arid northeastern region, Brazil

Douglas Alberto de Oliveira Silva[1], Suzana Maria Gico Lima Montenegro[2], Pabricio Marcos Oliveira Lopes[3], Jhon Lennon Bezerra Silva[1], José Ediclécio Barbosa dos Santos[1], Edvânia Matias da Silva[4], Adiel Felipe da Silva Cruz Correio[1], Wellington Manoel dos Santos[5], Sisgo Rachith Acuña Chinchilla[6], Ricardo Barros Silva[5], Dayane do Nascimento Cesar[4]

[1] Postgraduate Program in Agricultural Engineering, Department of Agricultural Engineering, Rural Federal University of Pernambuco. Av. D. Manoel de Medeiros, SN; Dois Irmãos, Recife, Pernambuco, Brazil. CEP: 52171-900. E-mail: douglasalbertosilva@hotmail.com (corresponding author); jhonlennoigt@hotmail.com; edicleciosantos@hotmail.com. [2] Water and Climate Resource Management Analyst, Agência Pernambucana de Águas e Clima - APAC. E-mail: suzana.ufpe@gmail.com.[3] Department of Agronomy, Rural Federal University of Pernambuco. Av. D. Manoel de Medeiros, SN; Dois Irmãos, Recife, Pernambuco, Brazil. CEP: 52171-900. E-mail: pabricio.lopes@ufrpe.br. [4] Post-Graduate Program in Agronomy / Plant Production, Department: Laboratory of Phytotechnics, Federal University of Alagoas, Center for Agricultural Sciences: Av. Manoel Severino Barbosa - Bom Sucesso, Arapiraca - AL, 57309-005. E-mail: dayanecesa@gmail.com. [5] Postgraduate Program in Agronomy/Plant Production, Department: Irrigation and Agrometeorology Laboratory, Federal University of Alagoas, Center for Agricultural Sciences: BR-104, Rio Largo - AL, 57100-000. E-mail: wellington.ea@hotmail.com; ricardoufal2010@gmail.com. [6] University: University of Costa Rica. Department: Escuela de Agronomía. Center for Agronomic Research (CIA), Rodrigo Facio University City, San José, Costa Rica. E-mail: rachith2001@yahoo.es.

Artigo recebido em 26/10/2019 e aceito em 20/07/2020

A B S T R A C T

Degradation of Caatinga biome has created desertification processes in several areas, inducing big microclimate and surface changes. Therefore, it is fundamental develop research methods capable of identifying areas under degradation process. Satellite images in different spatial, temporal, radiometric and spectral resolutions are being used to monitor big areas from several biomes worldwide. The objective of this study was to evaluate and quantify the degree of degradation and preservation of the Caatinga biome, using geoprocessing methods and remote sensing products, using surface data and Landsat-8 images for 2013, 2014 and 2015. Remote sensing methods were used to estimate the Normalized Difference Vegetation Index (NDVI), surface albedo (α) and Moving Standard Deviation Index (MDSI). The results showed that the vegetation indexes and the techniques of degradation and change detection satisfactorily identified the behavior of the surrounding vegetation in the study area, standing out as good indices for degradation processes in the semiarid. It was concluded that change detection and classification by decision tree methods were efficient in the identification of anthropized areas during the experimental period.

Key words: Caatinga, Decision tree, Degradation, NDVI, Remote Sensing.

Monitoreo de la degradación en el bioma de Caatinga en la región semiárida del Noreste de Brasil

Resumen

La degradación del bioma Caatinga ha creado procesos de desertificación en varias áreas, induciendo grandes cambios en el microclima y la superficie. Por lo tanto, es fundamental que se desarrollen métodos de investigación capaces de identificar áreas en proceso de degradación. Las imágenes de satélite con diferentes resoluciones espaciales, temporales, radiométricas y espectrales se están utilizando para monitorear grandes áreas de varios biomas en todo el mundo. El objetivo de este estudio fue evaluar y cuantificar el grado de degradación y preservación del bioma Caatinga, utilizando métodos de geoprocesamiento y productos de teledetección, usando datos de superficie e imágenes Landsat-8 para 2013, 2014 y 2015. Se utilizaron métodos de teledetección para estimar el Índice de Vegetación de Diferencia Normalizada (NDVI), el albedo de superficie (α) y el Índice de Desviación Estándar Móvil (MDSI). Los resultados mostraron que los índices de vegetación y las técnicas de monitoreo de la degradación y detección de cambios identificaron satisfactoriamente el comportamiento de la vegetación circundante en el área de estudio, destacándose como buenos

índices de los procesos de degradación en el semiárido. Se concluyó que los métodos de detección y clasificación de cambios por árbol de decisión fueron eficientes en la identificación de áreas antrópicas durante el período experimental.
Palabras clave: Árbol de decisión, Caatinga, Degradación, NDVI.

Introduction

Caatinga biome is exclusively found in Brazil, located mainly in the Northeastern region, with a small stand in the Southeastern region (north of Minas Gerais) (Silva et al., 2004; Silva et al., 2019; Cavalcante et al., 2020), comprising near 10% of the country's territory. The Caatinga, because it is anonly and exclusive Brazilian biome, needs to be conserved, considering a large amount of endemic plant and animal species. Regarding man-made degradation, the Caatinga is the third most degraded biome in Brazil, after Atlantic Forest and Cerrado (Myers et al, 2000; Pereira et al., 2017; Bezerra et al., 2020; Silva et al., 2020).

The monitoring with orbital imagery enables detecting, analyzing and inferring on Earth's surface shifts caused by natural or man-made processes (Leite et al., 2020). Several studies have been demonstrating that precipitation before the passage of satellites influences the spectral behavior of the vegetation cover of Caatinga. Bustamante et al. (2012) and Silva et al. (2019) observed direct relationship between the Caatinga annual growth and precipitation seasonality. Arraes et al. (2012) emphasized that the increase in NDVI is related to soil moisture content from prior months. Francisco et al. (2012) stated that precedent moisture content influences the spectral responses of Landsat-5 images and that vegetation type can be separated in Caatinga classes.

Several authors have developed research about the identification and quantification of environmental degradation in different regions of Brazil using Geographic Information System (GIS). Dias, Salvador, and Branco (2014), identified levels of declining in the riparian forests of the Southeast region using GIS. The authors determined the degree of degradation in the Water Resources Management Unit of Tietê-Jacaré, in the municipality of São Carlos-SP. In their study, Fernandes et al. (2009) sought to perform a space-time analysis of the degradation and the land cover and use in the semi-arid region of Sergipe, using Landsat-5 TM and Landsat-8 OLI (Operational Land Images) images during the years of 1992, 2003 and 2013.

Spectral heterogeneity may be processed using the Decision Tree (DT) method (Ruiz et al., 2014). The DT algorithm has been applied with success to several environmental evaluation studies. Xu et al. (2009) used NDVI, Moving Standard Deviation Index (MSDI) and surface albedo to evaluate and classify the degree of vegetation cover change in the Ordos Plateau in China, with Landsat 4, 5 and 7 images under regional scale. Ottinger et al. (2013) used the DT algorithm and Landsat-5 images to evaluate changes on land cover in urban and intensive farming areas from the Yellow River delta in China. Chasmer et al. (2014) merged spectral, elevation and vegetation structural attributes in order to classify land cover in a region with Permafrost.

The objective of this study was to evaluate and quantify the degree of degradation and preservation of the Caatinga biome, using geoprocessing methods and remote sensing products.

Material and Methods

Study area characterization

The study site comprises the area of Caatinga from Lagoa Grande-PE, located in the surrounding rectangle: (08º 48' 50 " S, 40º 30' 23" W; 09º 05' 42" S, 40º 18' 32" W; 08º 41' 39"S, 40° 11' 41"W; 09º 14' 03"S, 40º 11' 42"W, with average altitude of 220 meters above sea level) (Figure 1). This area is also part of the semiarid region of Northeastern Brazil.

Rain Anomaly Index (RAI) and weather data

Daily rainfall data of an Automated Meteorological Station (AMS) from a neighboring Municipality called Petrolina, located under 9º 22' 45.12''S and 40º 28' 47.25''W were made available by the Instituto Nacional de Meteorologia (www.inmet.gov.br) for the period of 2013 to 2015. Furthermore, annual total precipitation from 1993 to 2016 was used to select extreme precipitation years using the Rain Anomaly Index (RAI) proposed by Van Rooy (1965) and posteriorly adapted by Freitas (1998), in order to obtain positive and negative anomalies (Equations 1 and 2).

$$+RAI = 3 \times \left[\frac{N-\acute{N}}{\acute{M}-\acute{N}}\right] \quad (1)$$

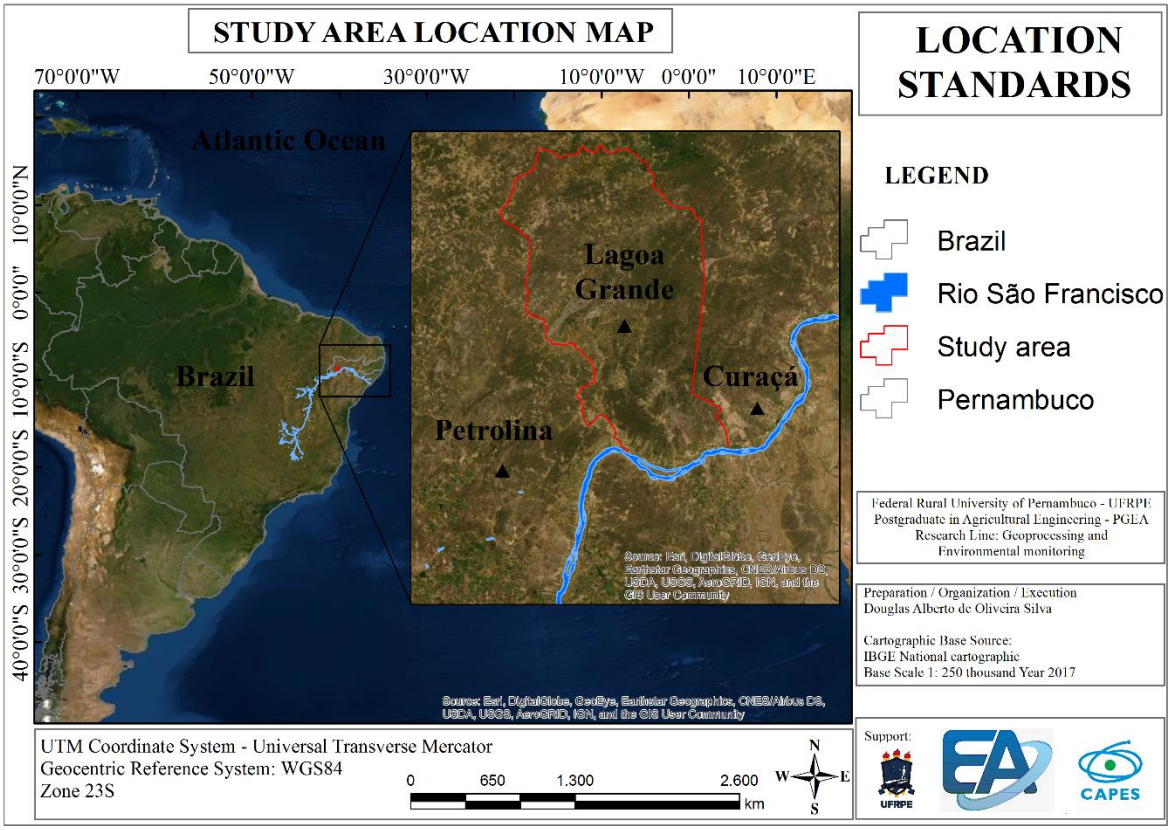

Figure 1. Location map of the study area.

$$-RAI = -3 \times \left[\frac{N-\acute{N}}{\acute{X}-\acute{N}}\right] \qquad (2)$$

In which: N = actual annual precipitation (mm), $\acute{N}$ = historical series average precipitation (mm), $\acute{M}$ – average from the ten greatest annual precipitations from the historical series (mm) and $\acute{X}$ = average from the ten lowest annual precipitations from the historical series (mm).

Table 1. Rainfall classification according to the RAI.

Rain Anomaly Index (RAI)	Rainfall classification
Bigger then 4	Extremely rainy (ER)
In between 2 and 4	Very rainy (VR)
In between 0 and 2	Rainy (R)
0	Neither Rainy nor Dry
In between 0 and -2	Dry (D)
In between -2 and -4	Very Dry (VD)
Less than -4	Extremely Dry (ED)

From the calculated values, the rainfall regime was classified according to RAI methodology presented in Table 1. This classification was elaborated by Van Rooy (1965) for dry and rainy years; such classification format uses the values recorded for RAI, as shown in Table 1.

Use and occupation of soil

The land use classification map of the study area was obtained from MapBiomas products through the platform http://platform.mapbiomas.org/map (Figure 2). This map allows to generate information about the dynamics, in time and space, of Caatinga area use and occupation.

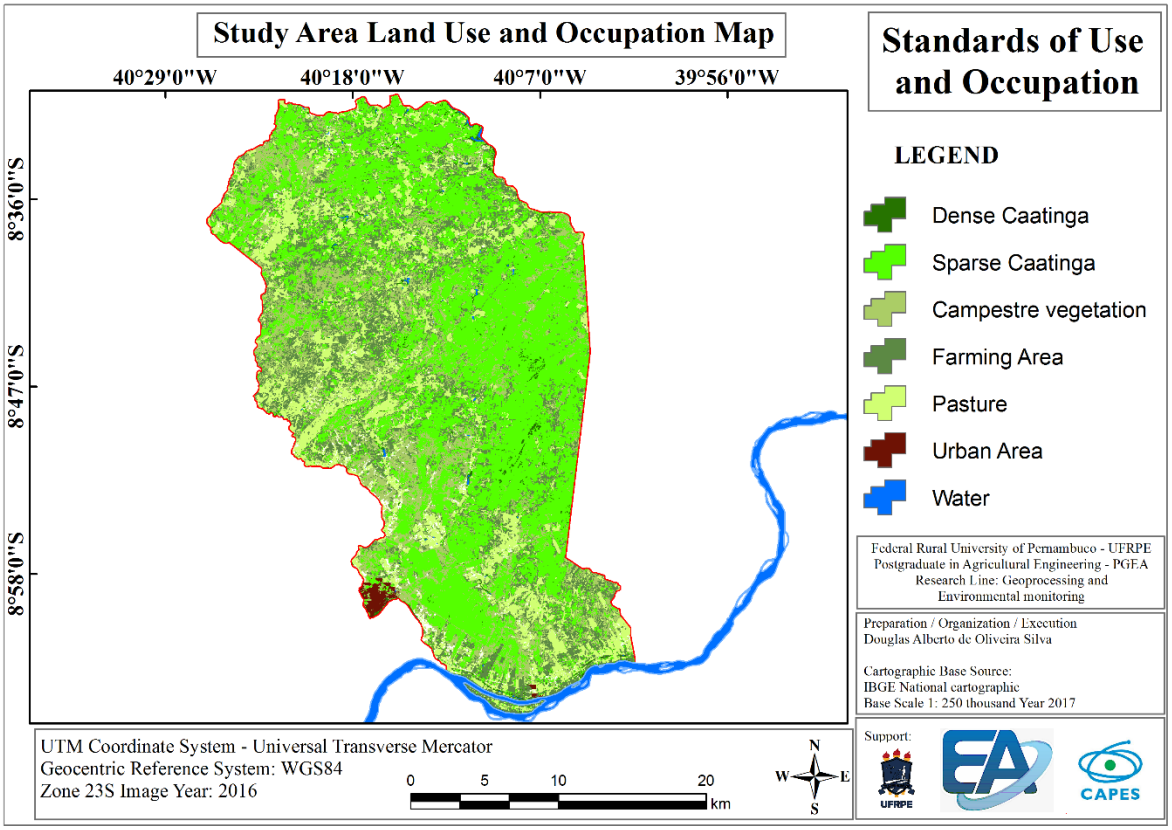

Figure 2. Map of soil use and occupation of the study area

Multispectral data processing and atmospheric correction

The images from Landsat-8 satellite were obtained on the United States Geological Survey website http://earthexplorer.usgs.gov/, with 30-m spatial resolution (bands 2 to 7) and radiometric resolution of 16 bits. Images covering study area, are fromorbit 217 and point 67. The following criteria were used to choose the images: clear sky conditions with the least cloud presence possible (<10%) and belonging to the same period of the year, passing over the study site around 09 h 45 min (local time).

Atmospheric correction of the images was performed using FLAASH (Fast Line-of-sight Atmospheric Analysis of Spectral Hypercubes) model (Cooley et al., 2002), by inputting date, hour, Landsat-8 passage location, tropical atmospheric model, continental aerosol and the horizontal atmospheric visibility (VIS) was estimated by inverting Equation 3 suggested by Deschamps et al. (1981).

$$\beta = 0.613 \times e^{-VIS/15} \quad (3)$$

In which: β = Ångström coefficient. It was considered a β equal to 0.18 for VIS of 18.26 km, optical depth of 0.08556 (www.patarnott.com), Ångström exponent of -1.3, atmospheric pressure of 973.44 mb, central wave length of band 3 (561.25 nm), latitude, longitude from the scene's middle point, date and time of Landsat-8 passage (Table 2).

Table 2. Meteorological variables from Lagoa Grande-PE on Julian day (JD) and passage hours of Landsat-8 are solar elevation angle (E), air temperature (T, °C), relative humidity (RH, %), atmospheric pressure (Po, hPa), optical depth (τ) and horizontal visibility (VIS, km).

Dates	JD	E	T	RH	Po	τ	VIS
30/05/2013	151	47.699	24.4	59	974.7	0.0856	18.23
09/03/2013	246	58.280	23.8	56	974.9	0.0857	18.23
10/05/2013	278	65.128	29.9	42	972.4	0.0855	18.26
06/02/2014	153	48.879	24.1	62	971.6	0.0856	18.28
08/05/2014	217	51.118	24.9	58	976.6	0.0860	18.20
09/22/2014	265	62.348	29.5	38	972.3	0.0854	18.26
08/24/2015	236	55.172	24.4	63	973.9	0.0856	18.25
10/27/2015	300	65.969	26.4	60	974.1	0.0857	18.26
11/12/2015	316	64.848	26.0	87	972.1	0.0855	18.26
12/14/2015	348	60.546	24.4	63	971.8	0.0850	18.37

Image Processing

Surface albedo (α), which represents the land capacity to reflect solar energy, was calculated according to Equation 4 (Silva et al., 2016).

$$\alpha = -62.2 \times \rho_2 - 57.3 \times \rho_3 - 48.3 \times \rho_4 - 29.5 \times \rho_5 - 7.3 \times \rho_6 - 2.4 \times \rho_7 \quad (4)$$

In which ρ_2, ρ_3, ρ_4, ρ_5, ρ_6 and ρ_7 of reflectance of each band of Landsat-8.

The NDVI indicates the degree of photosynthetic of healthy vegetation estimated by Equation 5.

$$NDVI == \frac{\rho_5 - \rho_4}{\rho_5 + \rho_4} \quad (5)$$

The MSDI corresponds to the standard deviation calculated through a 3 × 3 filter applied to band 4 of Landsat-8, according to Equation 6.

$$MSDI = \sqrt{\frac{\sum_{i=1}^{n} (DN_i - \overline{DN_i})^2}{N}} \quad (6)$$

in which: N = number of pixels from the 3x3 filter, herein N = 9; DN_i = pixel value; $\overline{DN\imath}$= average digital number value of each 9-pixel window.

Environmental degradation thematic maps from Caatinga biome area were estimated from DT classification. The rule sets of indicators for each environmental classification class are listed in Table 3, in accordance with Xu et al. (2009). The study site shows great heterogeneity, which in turn was fundamental to define the degradation status on a regional scale. Non-existent degradation classes, low and severe degradation, were accurately identified using only NDVI and surface albedo. The MSDI was mainly used to distinguish average and high degradation.

Table 3. Rule set for degradation evaluation, using Landsat-8 images. Source: Adapted from Silva et. al (2019).

Degradation Classes	NDVI	MSDI	Albedo
Non-existent	< 0.25	---	< 0
	< 0.50	---	---
	< 0		
Low	< 0.25	---	> 0
Average	0.32 < e < 0.40	> 3	0.175 < e < 0.19
	0.32 < e < 0.40	< 3	0.175 < e < 0.19
High	0.25 < e < 0.32	> 3	0.175 < e < 0.19
	0.25 < e < 0.32	< 3	0.175 < e < 0.19
Severe	< 0.25	---	> 0.22

In order to evaluate the classifiers' precision on generating the thematic maps, the Kappa Index was used together with accuracy. Table 4 presents the performance levels of classification for the obtained Kappa value, Galparsoro and Fernández (2001).

Table 4. Kappa index and the corresponding classification performance.

Kappa	Performance
< 0	Terrible
0 < k ≤ 0.2	Bad
0.2 < k ≤ 0.4	Reasonable
0.4 < k ≤ 0.6	Good

Source: Adapted from Galparsoro and Fernández (2001).

Land use and occupation change intensity (A) was calculated from the values of band 4 and 5 reflectances in time 1 (actual month) and time 2 (subsequent month to the actual one) expressed by the Equation 7 (Zhan et al., 2000).

$$A = \sqrt{(\Delta\rho_4)^2 + (\Delta\rho_5)^2} \quad (7)$$

Results and discussion

Figure 3 shows the annual RAI values for the studied station. It was observed a 4-year period of drought between the consecutive years of 2010 and 2013; and two 2-year periods of drought: a weak one between 2006 and 2007; and a strong one between 2015 and 2016. In addition, it was observed a 3-year period of rainfall for the consecutive years of 1994 to 1996; and two 2-year periods of consecutive rainy years, that is, a weak period between 1999 and 2000, and a strong one between 2008 and 2009. The values calculated for annual RAI ranged from -4.929 and + 5.026. Alves

et al. (2016), when studying the city of Petrolina from 1964 to 2007, have found RAI value ranging from -5.31 and +7.24.

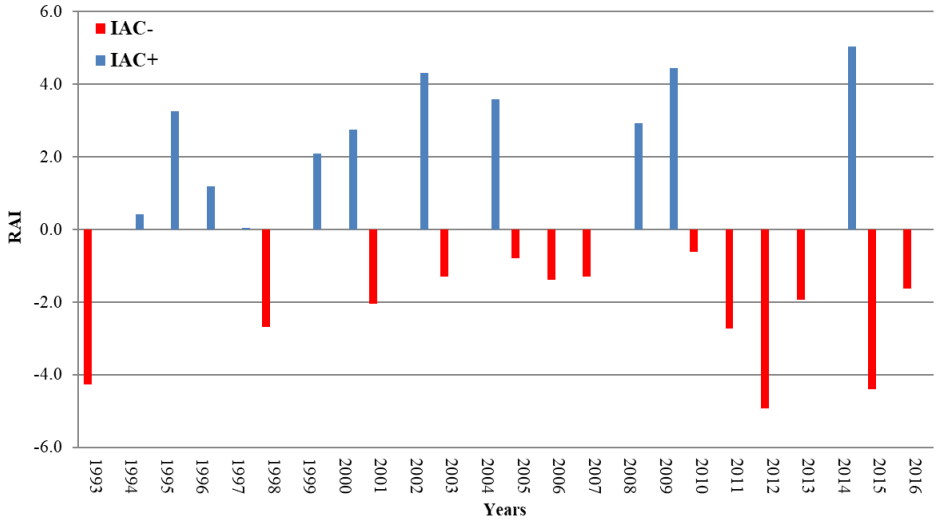

Figure 3. Annual RAI of the studied station for the consecutive period of 1993 to 2016.

Through visual analysis, a reduction trend on RAI values was observed for the last few years, except for 2014, but negative anomalies frequency is greater than the positive ones. Such RAI variability is related to the influence of the Atlantic Dipole phenomenon and anomalous events in the Pacific Ocean associated to El Niño-South Oscillation (Oliveira Júnior et al., 2012; Alves et al., 2016; Silva et al., 2017).

Figure 4 shows the spatial and temporal variabilities of land surface albedo (α) related to land use and occupation in the Caatinga biome area. From the studied scenes, vegetation areas, such as Caatinga and irrigated fruit farming fields, present α from 0% to 8%. These values are explained by the crop development and the change in light incidence angle on vegetation canopy surface (Leitão et al., 2002). Silva et al. (2005), studied the α in Petrolina-PE and noted that fruit farming areas showed nearly constant values, around 15%, which is greater than this study.

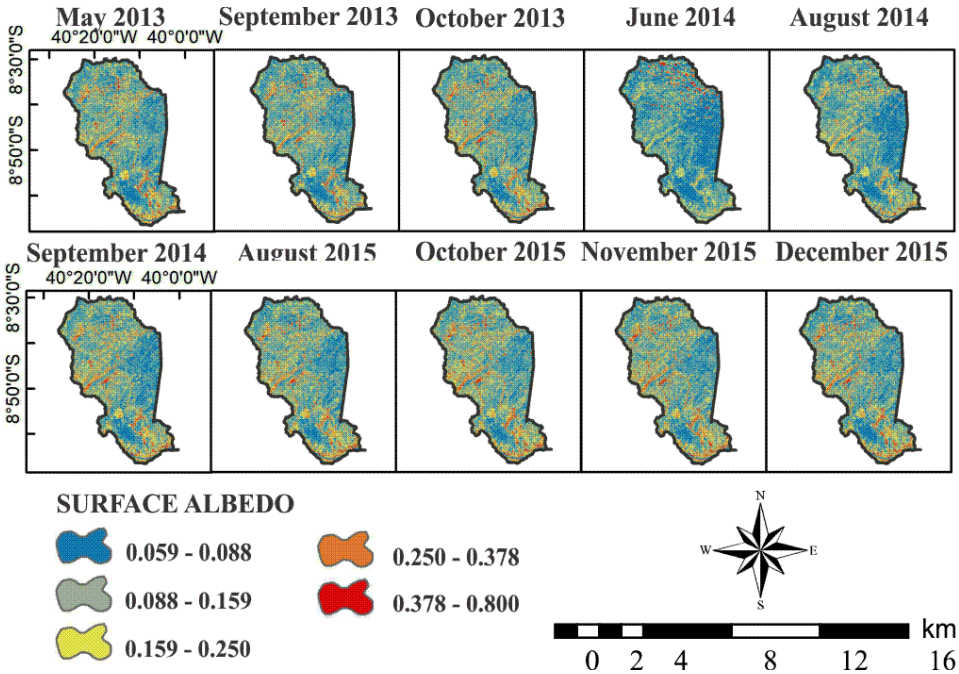

Figure 4. Temporal and spatial evaluation of the surface albedo in the Caatinga biome area.

On bare soil areas, α variation from 2013 to 2015 ranged from 37% to 80%. Land surface albedo controls the amount of solar energy that is absorbed by the Earth's surface, thus plays an important role as a radiation balance modulator to the surface (Arraes et al., 2012). The α values in urban zones vary from 8% to 80%, is considered a high amplitude variation within the studied period. It can also be verified that the Sobradinho embankment, as well as São Francisco riverbank, show a blue hue with α values lower than 8% (Figure 4).

Corroborating the results from Silva et al. (2019), who computed land surface albedo with OLI-Landsat 8 in the Brazilian semiarid and found albedo values for June, September and October 2013, their results showed that areas with albedo lower than 9% comprise bodies of water (São Gonçalo dam and small lakes, rivers, and creeks). Urban areas, in general, present albedo values greater than 25%, which is also observed in bare soil. Irrigated crop fields within São Gonçalo irrigation perimeter showed albedo from 16% to 18%; however, newly planted orchards (low vegetation index), greater soil exposure caused an albedo value increase.

In Figures 5A and 5D, the vegetation has great photosynthetic activity when compared to the other images. This behavior is due to rainfall collection in the Caatinga biome area during the 3 months prior to imaging. On the other hand, low precipitation levels before imaging on 05/10/2013 AMS=17.6 mm; 09/22/2014 AMS=35.9 mm; 08/24/2015 AMS=5.1 mm; 10/27/2015 AMS=13.8 mm and 12/14/2015 AMS=17.3 mm lead to greater foliage of Caatinga deciduous plant species.

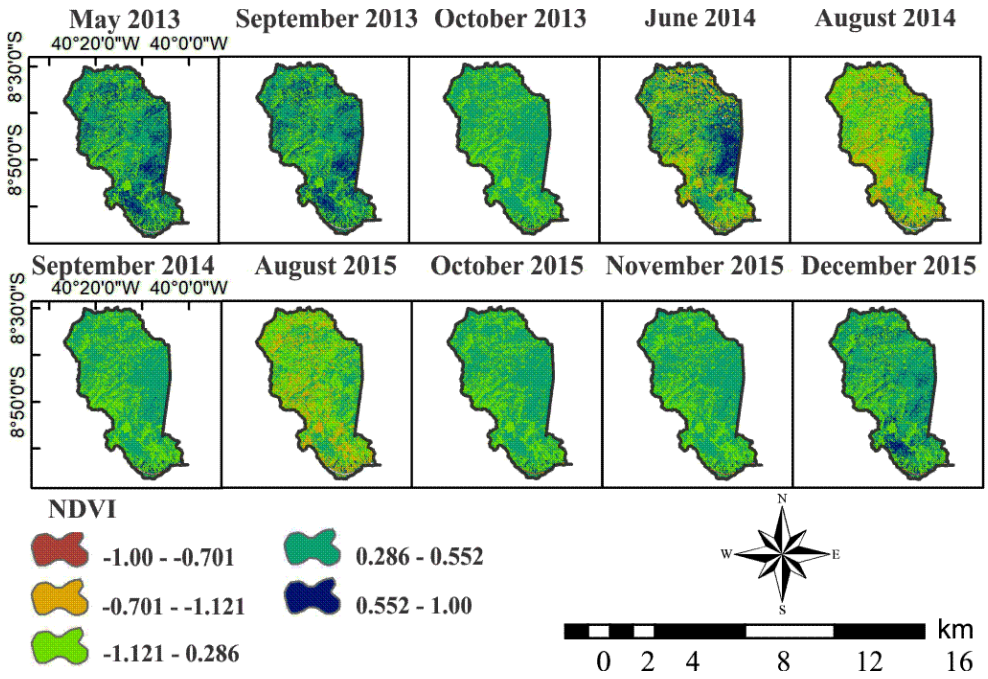

Figure 5. Temporal and spatial evaluation of the NDVI in the Caatinga biome area.

The greatest mean NDVI values for native vegetation areas are recorded in the image for June 2014 (Figure 5), when compared to the values from the other images. The imaging period (June) matches the rainy season, when there are a great herb layer and significant presence of vegetation leaf canopy, thus contributing to higher NDVI levels. Another important factor that should be considered in the Caatinga environment is the seasonal rainfall distribution, which plays a great role on the regional water balance, hence soil moisture content, thus directly influencing NDVI (Arraes et al., 2012; Silva Filho et al., 2020).

During May and September 2013, June 2014 and December 2015, there is high spatial and temporal variability of vegetation cover (Figure 5) with NDVI values for irrigated area from 0.55 to 1; Caatinga from 0.12 to 0.55; bare soil equal to 0.07, 0.098 and 0.075; urban area equal to 0.014, 0.016 and 0.013, respectively. Souza (2016), has found lower values for bare soil (0.01), and urban area (0.02 and 0.03) for João Pessoa in Paraíba state, which was proportional to the precipitation.

Generally, mean NDVI values ranged from the lowest 0.29 in December 2015 to the highest 0.55 in June 2014 (Figure 5), corroborating Ferreira et al. (2012), who observed mean NDVI values between 0.28 and 0.36 for the year 2011 in Petrolina-PE. Oliveira (2012) observed mean NDVI values ranging from 0.35 to 0.73.

Table 5 shows the accuracy and confidence level of the degradation maps with the used classes, through accuracy and Kappa Index analysis. It may be verified though accuracy values (Table 5) that the classification results were satisfactory with a mean accuracy value of 98.49%, greater precision was found on 05/10/2013, 06/02/2014 and 08/05/2014 with accuracy value of 99.96%. Another statistic test applied to the classification results, which was related to the confusion matrix, and represents the disagreements in classification was the Kappa Index estimation. Regarding Kappa values, it was observed an average of 0.97; the greatest value was 0.99 on 05/10/2013, 30/05/2013 and for all images 2014, while the lowest value was 0.88 on 08/24/2015.

Table 5. Kappa index and Accuracy values in Caatinga biome area from 2013, 2014 and 2015.

Dates	Kappa	Accuracy
30/05/2013	0.99	99.76
09/03/2013	0.98	99.16
05/10/2013	0.99	99.96
06/02/2014	0.99	99.96
08/05/2014	0.99	99.96
09/22/2014	0.99	99.41
08/24/2015	0.88	92.99
10/27/2015	0.96	97.67
11/12/2015	0.95	97.07
12/14/2015	0.99	98.92

Based on Table 5, the total values for the Kappa Index found were considered excellent for every image. Mishra, Arman Rai and Chand Rai (2019) using geospatial techniques to detect changes in the Rani Khola river basin, from 1988 to 2017, obtaining an average Kappa index of 0.81 in 2017, which is lower than that currently in work. Demarchi et al. (2011), using Landsat-5 images, analyzed surface changes and obtained Kappa values well below the ones found in this study, from 0.57 to 0.74, which are good and very good classifications, respectively.

The great accuracy for image classification, by using Kappa Index, may be explained by the high heterogeneity observed in the study site, which in turn is related to the spectral difference existent between targets. However and Oliveira et al. (2015), observed opposite results when mapping forests with images from TM/Landsat 5 and RapidEye.

Results for the evaluation from 2013 to 2015 are shown in Figure 6. Although some regions of the study site have shown expansion of the degradation process, overall there is a reversal trend. This behavior is observed when analyzing the degradation maps for May, September and October 2013 (Figure 6), between May and October there was an increase on the decline process, mainly for medium and high classes, but it was observed a reduction in October. On the other hand, there is a sharp increase in June and August 2014, with a lesser number of non-existent degradation regions and the greater number of medium class regions. Similar results were obtained by Silva et al. (2019) when estimating environmental degradation in the Caatinga region using geospatial data. Wang et al. (2004), analyzing surface degradation in Northern China between 1988 and 2000, have used a similar classification method, thus corroborating the present study.

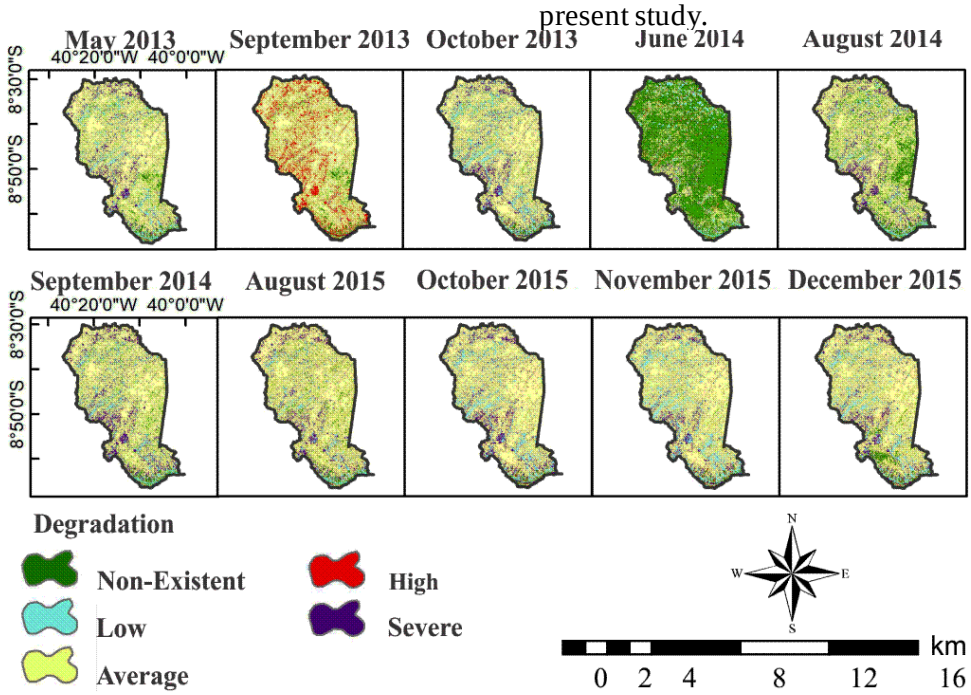

Figure 6. Temporal and spatial evaluation of the degradation in the Caatinga biome area.

The map for June 2014 (Figure 6) shows that there is no degradation for most of the map. Such class, which comprises the values that do not pose soil degradation risk, present the representative sectors. Among these observations, it can be inferred that during the imaging date the study site holds the lowest degradation risk. It can also be observed in Figure 6 that the purple hue regions, which correspond to the severe degradation class and represents pixels with the lowest NDVI values and the highest albedo and MSDI values, match mainly urban areas, bare soil areas and salt-affected areas with high desertification susceptibility. It is noteworthy to point out that the degradation process is centered in the São Francisco river and neighboring areas, as well as near anthropized areas, due to Caatinga suppression and irrigated areas withdrawal.

The results of the evaluation of the magnitude changes on land use and occupation from 2013 to 2015 are shown in Figure 7. It is observed that the imaging of the scenes from 2013, when compared to the next years, have shown greater areas under severe degradation class (red hue), indicating man-made processes of the study site which leads to soil and vegetation degradation. Between the previous month (September 2013) and the following month (October 2013), rainfall precipitation was only 4.6 mm, which is considered below average for both months. Zhan et al. (2000), have also associated precipitation events as the main factor for the presence of more severe class in a given area.

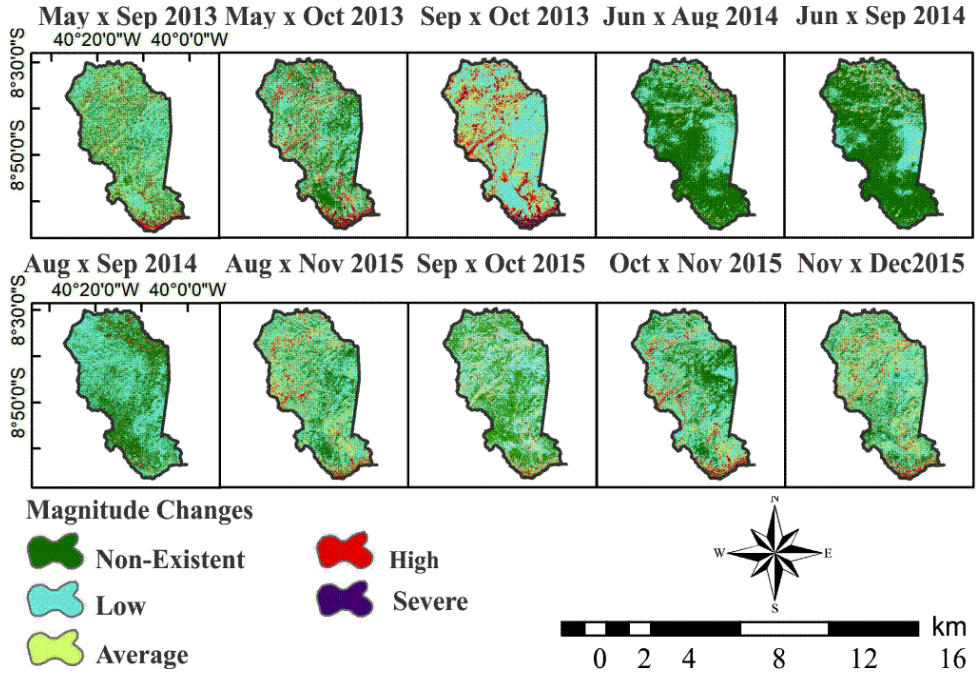

Figure 7. Temporal and spatial evaluation of the magnitude changes in the Caatinga biome area.

By comparing the results (Figure 7), it is notable that there is a similarity between the images from 2014, predominating areas with no degradation. This behavior is explained, in part, by the fact that 2014 had a "normal" rainfall regime when compared to 2013 and 2015 since Caatinga biome has great resilience. Its response to rainfall events is rapid, therefore there was a recovering of Caatinga foliage after a 30-mm rainfall during the period in which the images were compared (June to August) in Caatinga biome area.

The changes in land use and occupation were identified by the decrease of vegetation indices and the increase in albedo values. The indexes used in this study satisfactorily identified vegetation status in the Caatinga biome area, standing out as indices for degradation processes in semiarid regions. The methods of change magnitude and degradation quantification by decision tree are efficient for the monitoring of environmental degradation and soil cover alterations, throughout the three years, showing high values of Kappa index and accuracy.

Acknowledge

The authors would like to thank the reviewers for their corrections and suggestions; CAPES for the granting of a master's degree and the Postgraduate Program in Agricultural and Environmental Engineering of UFRPE for the opportunity to hold the doctorate.

References

Alves, J.O., Pereira, P.C., Queiroz, M.G., Silva, T.G.F, Ferreira, J.M.S., Araújo Júnior, G.N., 2016. Índice de anomalia de chuva para diferentes mesorregiões do Estado de Pernambuco, Journal Thinking Academic. 14, 37-47. Disponível https://doi.org/10.21576/rpa. 2016v14i1.4. Acesso: 23 jun. 2019.

Arraes, F.D.D., Andrade, E.M., Silva, B.B., 2012. Dinâmica do balanço de energia sobre o açude Orós e suas adjacências, Journal Caatinga. 25, 119-127. Acesso: 23 jun. 2019.

Bezerra, A.C., Silva, J.L.B., Silva, D.A.O., Batista, P.H.D., Pinheiro, L.C., Lopes, P.M.O., Moura, G.B.A. Monitoramento Espaço-Temporal da Detecção de Mudanças em Vegetação de Caatinga por Sensoriamento Remoto no Semiárido Brasileiro. Revista Brasileira de Geografia Física. 01, 286-301. Disponível: 10.26848/rbgf.v13.1.p286-301. Acesso: 17 jul. 2020. 2020.

Bustamante, M.M., Nobre, C.A., Smeraldi, R., Aguiar, A.P, Barioni, L.G., Ferreira, L.G., Longo, K., May, P.,.Pinto, A.S., Ometto J.P., 2012. Estimating greenhouse gas emissions from cattle raising in Brazil, Climatic Change. 115, 559-577. Doi:10.1007/s10584-012-0443-3. Acesso: 24 jun. 2019.

Cavalcante, W.F., Silva, L.R.C.D., Silva, E.G.D., Oliveira, J.T.C., & Moreira, K.A. Enzymatic activity of Caatinga biome with and without anthropic action. Revista Caatinga, 33, 142-150. https://doi.org/10.1590/1983-21252020v33n116rc. Acesso: 14 jul. 2020.

Chasmer, L., Hopkinson, C., Veness, T., Quinton, W., Baltzer. J., 2014. A decision-tree classification for low-lying complex land cover types within the zone of discontinuous permafrost, Remote Sensing of Environment. 143, 73-84. https://doi.org/10.1016/j.rse.2013. 12.016. Acesso: 26 jun. 2019.

Cooley, T., Anderson, G.P., Felde, G.W., Hoke, M.L., Ratkowski, A.J., Chetwynd, J.H., Gardner, J.A., Adler-Golden, S.M., Matthew, M.W., Berk, A., Bernstein, L.S., Acharya, P.K., Miller, D., Lewis. P., 2002. FLAASH, a MODTRAN4-based atmospheric correction algorithm, its application and validation. IEEE International Geoscience and Remote Sensing Symposium, 3, 1414-1418. Disponível: DOI:10.1109/IGARSS.2002.1026134. Acesso: 26 jun. 2019.

Demarchi, J.C., Piroli, E.L., Zimback, C.R.L., 2011. Análise Temporal do Uso do Solo e Comparação Entre os Índices de Vegetação NDVI E SAVI no Município de Santa Cruz do Rio Pardo – SP Usando Imagens Landsat-5, Raega - The Geographic Space in Analysis. 21, 234-271, Disponível: DOI: http://dx.doi.org/10. 5380/raega.v21i0.17416. Acesso: 11 jun. 2019.

Dias, R.M., Salvador, N.N.B., Branco. M.B.C., 2014. Identificação dos Níveis de Degradação de Matas Ripárias com o Uso de SIG. Revista Floresta e Ambiente. 21, 150-161. Disponível: http://dx.doi.org/10.4322/floram.2014.032. Acesso: 26 ago. 2019.

Fernandes, M.R.M., Matricardi, E.A.T., Almeida, A.Q., Fernandes. M.M., 2015. Mudanças do Uso e de Cobertura da Terra na Região Semiárida de Sergipe, Revista Floresta e Ambiente. 21, 150-161. Disponível: http://dx.doi.org/10.1590/2179-8087.121514. Acesso: 16 set. 2019.

Ferreira, J.M.S., Ferreira, H.S., Silva, H.A., Santos, A.M., Galvíncio. J.D., 2012. Análise espaço-temporal da dinâmica da vegetação de Caatinga no Município de Petrolina – PE, Brazilian Journal of Physical Geography. 5, 904-922, https://doi.org/10.26848/rbgf.v5.4.p904-922. Acesso: 06 set. 2019.

Francisco, P.R.M., Chaves, I.B., Lima, E.R.V., Bandeira, M.M., Silva. B.B., 2012. Mapeamento da Caatinga com Uso de Geotecnologia e Análise da Umidade Antecedente em Bacia Hidrográfica, Brazilian Journal of Physical Geography. 5, 676-693. https://doi.org/ 10.26848/rbgf.v5.3.p676-693. Acesso: 22 set. 2019.

Freitas, M.A.S., 1998. Um sistema de suporte à decisão para o monitoramento de secas meteorológicas em regiões semiáridas, Journal Technology. 19, 84-95. Disponível: http://dx.doi.org/10.5020/23180730.1998.1175 Acesso: 26 jun. 2019.

Galparsoro, L.U., Fernández, S.P., 2001. Medidas de concordancia: el índice Kappa.

Leitão, M.M.V.B.R., Santos, J.M., Oliveira, G.M., 2002. Estimativas do albedo em três ecossistemas da floresta amazônica, Revista Brasileira de Engenharia Agrícola e Ambiental. 6, 256-261. Disponível: http://dx.doi.org/10. 1590 /S1415-43662002000200013. Acesso: 17 abr. 2019.

Leite, C.R.M., Lopes, P.M.O., Nascimento, C.R., Moura, G.B.A., Silva, D.A.O., Silva, J.L.B. Semi-aridity nuclei associated the land cover and soil moisture in Pernambuco, Brazil. Journal of Hyperspectral Remote Sensing. 01, 20-33. Disponível: https://doi.org/10.29150/ jhrs.v10.1.p20-33. Acesso: 17 jul. 2020. 2020.

Mishra, P.K., Rai, A., & Rai, S.C. Land use and land cover change detection using geospatial techniques in the Sikkim Himalaya, India. The

Egyptian Journal of Remote Sensing and Space Science. https://doi.org/10.1016/j.ejrs.2019.02.001 Acesso: 14 jul. 2020. 2019.

Myers, N., Mittermeier, R.A., Mittermeier, G.A., Fonseca, B., KENT. J., 2000. Biodiversity hotspots for conservation priorities, Nature. 403, 853-858. Acesso: 17 abr. 2019.

Oliveira, C.P., 2015. Modelagem dinâmica da cobertura florestal do Município de Floresta – PE. 68f. Dissertation (Master in Forestry Sciences), Rural Federal University of Pernambuco, Recife, PE.

Oliveira Júnior, J.F., Lyra, G.B., Góis, G., Brito, T.T., Moura. N.S.H., 2012. Análise de homogeneidade de séries pluviométricas para determinação do Índice de Seca IPP no Estado de Alagoas, Journal Forest and Environment. 19, 101-112. Disponível: http://dx.doi.org/10.4322/floram.2012.011. Acesso: 17 abr. 2019.

Ottinger, M., Kuenzer, C., Liu, G., Wang, S., Dech, S., 2013. Monitoring land cover dynamics in the Yellow River Delta from 1995 to 2010 based on Landsat 5 TM, Applied Geography. 44:53-68. Disponível: https://doi.org/10.1016/j.apgeog.2013.07.003. Acesso: 17 abr. 2019.

Pereira, J.S., Moraes Neto, J.M., Firmino, M.C., Fernades, M.F., Silva, M.J., 2017. Análise espaço temporal da cobertura vegetal no Município de Taperoá - PB, Brasil, Revista Espacios. 38, 5. Acesso: 17 jul. 2019.

Ruiz, L.F.C., Ten Caten, A., Dalmolin, R.S.D., 2014. Árvore de decisão e a densidade mínima de amostras no mapeamento da cobertura da terra. Journal of Rural Science. 44, 1001-1007. Disponível: DOI: 10.1590/S0103-84782014000600008. Acesso: 17 jul. 2019.

Silva, M.F., 2016. Uma análise do bioma caatinga no Município de Gado Bravo - PB através do Índice Vegetação por Diferença Normalizada. 52f. Dissertation (Master in Environmental Science and Technology) – State University of Paraíba, Campina Grande, PB.

Silva, D.A.O., Lopes, P.M.O., Moura, G.B.A., Silva, E.F.F., Silva, J.L.B., Bezerra, A.C., 2019. Evolução Espaço-Temporal do Risco de Degradação da Cobertura Vegetal de Petrolina-PE. Revista Brasileira de Meteorologia. 34, 1-11. Disponível: http://dx.doi.org/10.1590/0102-7786334018. Acesso: 18 jul. 2019.

Silva, A.R., Santos, T.S., Queiroz, D.E., Gusmão, M.O., Silva, T.G.F., 2017. Variações no índice de anomalia de chuva no semiárido, Journal of Environmental Analysis and Progress. 2, 377-384. Disponível: 10.24221/jeap.2.4.2017.1420. Acesso: 22 set. 2019.

Silva, J. L. B., Moura, G.B.A., Lopes, P.M.O. Spatial-Temporal Monitoring of the Risk of Environmental Degradation and Desertification by Remote Sensing in a Brazilian Semiarid Region. Revista Brasileira de Geografia Física, 02, 544-563. Disponível: 10.26848/rbgf.v13.2.p544-563. Acesso: 17 jul. 2020. 2020.

Silva, B.B., Lopes, G.M., Azevedo, P.V., 2005. Determinação do albedo de áreas irrigadas com base em imagens Landsat 5-TM, Brazilian Journal of Agrometeorology. 13, 201-211.

Silva, J.M.C., Tabarelli, M., Fonseca, M.T., Lins, L.V., 2004. Biodiversidade da Caatinga: áreas e ações prioritárias para a conservação. 382 f. Ministry of the Environment, Brasília, DF.

Silva Filho, R., Vasconcelos, R.S., Oliveira G.C., Cunha, J.E.D.B.L., Rufino, I.A.A. Representação matemática do comportamento intra-anual do NDVI no Bioma aatinga. Ciência Florestal, 30, 473-488. Acesso: 14 jul. 2020. 2020.

Souza, J.F., Silva, R.M., Silva, A.M., 2016. Influência do uso e ocupação do solo na temperatura da superfície: o estudo de caso de João Pessoa – PB. Journal Built Environment. 16, 21-37. Disponível: http://dx.doi.org/10.1590/s1678-86212016000100058. Acesso: 22 set. 2019.

Van Rooy, M.P.A., 1965. Rainfall anomaly index independent of time and space, Notes. 14, 43-48. Acesso: 22 set. 2019.

Wang, T., Wu, W., Xue, X., Sun, Q., Chen. Q., 2004. Study of spatial distribution of sandy desertification in North China in recent 10 years, Science in China Series D: Earth Sciences. 47, 78-88. Acesso: 22 set. 2019.

Xu, D., Kang, X., QIU, D., Zhuang, D., Pan, J., 2009. Quantitative Assessment of Desertification Using Landsat Data on a Regional Scale: A Case Study in the Ordos Plateau, China, Sensors. 9, 1738-1753. Disponível: DOI: 10.3390/s90301738. Acesso: 22 set. 2019.

Zhan, X., Defries, R., Townshend, J.R.G., Dimiceli, C., Hansen, M., Huang, C., Sohlberg, R., 2000. The 250 m global land cover change product from the Moderate Resolution Imaging Spectroradiometer of NASA's Earth Observing System, International Journal of remote sensing. 21, 1433-1460. Disponível: https://doi.org/10.1080/014311600210254. Acesso: 20 set. 2019.